Proton Transfer in Water Wires in Proteins: Modulation by Local Constraint and Polarity in Gramicidin A Channels

Shasikala Narayan,* Debra L. Wyatt,† David S. Crumrine,* and Samuel Cukierman†
*Department of Chemistry, Loyola University Chicago, Chicago, Illinois 60626; and †Department of Physiology, Loyola University Medical Center, Maywood, Illinois, 60153.

ABSTRACT The transfer of protons in membrane proteins is an essential phenomenon in biology. However, the basic rules by which H^+ transfer occurs in water wires inside proteins are not well characterized. In particular, the effects of specific atoms and small groups of atoms on the rate of H^+ transfer in water wires are not known. In this study, new covalently linked gramicidin-A (gA) peptides were synthesized, and the effects of specific atoms and peptide constraints on the rate of H^+ transfer were measured in single molecules. The N-termini of two gA peptides were linked to various molecules: S,S-cyclopentane diacid, R,R-cyclopentane diacid, and succinic acid. Single-channel proton conductances (g_H) were measured at various proton concentrations ($[H^+]$) and compared to previous measurements obtained in the S,S- and R,R-dioxolane-linked as well as in native gA channels. Replacing the S,S-dioxolane by an S,S-cyclopentane had no effects on the g_H-$[H^+]$ relationships, suggesting that the constrained and continuous transition between the two gA peptides via these S,S linkers is ultimately responsible for the two- to fourfold increase in g_H relative to native gA channels. It is likely that constraining a continuous transition between the two gA peptides enhances the rate of H^+ transfer in water wires by decreasing the number of water wire configurations that do not transfer H^+ at higher rates as in native gA channels (a decrease in the activation entropy of the system). On the other hand, g_H values in the R,R-cyclopentane are considerably larger than those in R,R-dioxolane-linked gA channels. One explanation would be that the electrostatic interactions between the oxygens in the dioxolane and adjacent carbonyls in the R,R-dioxolane-linked gA channel attenuate the rate of H^+ transfer in the middle of the pore. Interestingly, g_H-$[H^+]$ relationships in the R,R-cyclopentane-linked gA channel are quite similar to those in native gA channels. g_H values in succinyl-linked gA channels display a wide distribution of values that is well represented by a bigaussian. The larger peaks of these distributions are similar to g_H values measured in native gA channel. This observation is also consistent with the notion that constraining the transition between the two β-helical gA peptides enhances the rate of H^+ transfer in water wires by decreasing the activation entropy of the system.

INTRODUCTION

The translocation of protons in membrane proteins is an essential foundation of life. Energy generation (ATP synthesis), acid-base equilibrium, motility of bacteria, and synaptic transmission are but a few essential phenomena in which H^+ translocation plays decisive roles (1–3). Despite of its relevance, much remains to be learned about the basic rules by which H^+ are transferred across biological membranes and proteins.

The mobility or conductivity of H^+ in water is larger than of any other ion (4). In relatively dilute solutions, protons do not diffuse hydrodynamically as with other ions (with the notable exception of OH^-, which can also be regarded as a proton transfer mechanism) but are transferred by a mechanism that became known as Grotthuss's (see Cukierman (2) for a historical discussion of this phenomenon) (5–8). It was proposed that H^+ are transferred along a chain of H-bonded water molecules (water or proton wires (9)) as a consequence of an extensive reorganization of covalent OH bonds and H bonds between water molecules (5–11). Two coupled processes underlie these structural reorganizations. First, one H^+ is transferred between adjacent water molecules via hopping steps. If other H^+ are to be transferred in the same direction, water molecules need to rotate back (turn step) close to their original positions to accept another H^+. The rate-limiting step of the Grotthuss's mechanism in bulk water has been historically attributed to the turn step (6–9). This rate-limiting step for H^+ transfer in bulk water has been cogently questioned (10), and a significantly better understanding of this phenomenon is being developed (12–15). Although a classical Grotthuss's mechanism is not likely to occur in bulk water, such a mechanism could well be responsible for H^+ transfer in unidimensional water wires inside protein cavities (1,2,4,9).

Gramicidin A (gA) is a highly hydrophobic pentadecapeptide secreted by *Bacillus brevis*. It consists of an alternating sequence of D- and L-amino acids (HCO-L-Val-Gly-L-Ala-D-Leu-L-Ala-D-Val-L-Val-D-Val-(L-Trp-D-Leu)$_3$-L-Trp-NH-(CH$_2$)$_2$-OH). This primary structure defines in various molecular environments a right-handed single-stranded $\beta^{6.3}$-helix (16–20). Single gA peptides partition into distinct monolayers of a lipid bilayer. A functional ion channel is formed when two gA peptides located in opposite

Submitted March 19, 2007, and accepted for publication May 7, 2007.

Address reprint requests to Dr. Samuel Cukierman, Dept. of Physiology, Loyola University Medical Center, 2160 South First Ave., Maywood, IL 60153. E-mail: scukier@lumc.edu.

Editor: Meyer B. Jackson.

0006-3495/07/09/1571/09 $2.00

doi: 10.1529/biophysj.107.109231

monolayers of a bilayer associate their amino termini via six intermolecular H bonds in the middle of the membrane (17–20). Disruption of these H-bonds caused by fluctuations in the membrane-protein complex leads to the dissociation of peptides with loss of ion channel function (17–20).

The gA channels have an internal diameter and length of ~4 Å and 25 Å, respectively. These channels are selective for monovalent cations (21–23). Of particular significance for this study is that the lumina of gA channels contain a basically unidimensional water chain comprised of ~8–10 waters (24,25). A quite common observation in molecular dynamics studies of water wires in gA channels is that one of the hydrogens of a water molecule in the water wire donates an H-bond to a carbonyl group that projects into the pore of gA channel while the other water hydrogen donates an H bond to the oxygen of the adjacent water molecule (26–28). Thermal fluctuations in this H-bonded network of (gA plus water wire) must have a profound influence on the rate of transfer of H^+ in gA channels (26–28).

Relatively simple experimental molecular models to investigate the properties of proton transfer in water wires in gA channels have been developed in our laboratories in recent years. Initial molecules consisted of covalently linking native gA peptides to the S,S- and R,R-dioxolanes (4,29–32). Because of the marked differences in the arrangements of intra- and intermolecular H bonds in the channel wall between these molecules (27,30,33) and between them and native gA channels, it was reasoned and later demonstrated that the H^+ transfer properties in these channels were also remarkably distinct (4,29–31). Measurements of g_H values in these channels under a variety of experimental conditions support the conclusion that H^+ transfer (and not hydrodynamic flow of a solvated proton) may well be occurring in gA channels (1,2,34,35).

The objective of this study was to experimentally probe the structural or atomic basis for the functional differences in the rates of H^+ translocation between the native and the S,S- and R,R-dioxolane-linked gA channels (4,30). This was accomplished by replacing specific atoms in the dioxolane linker and modifying or releasing the molecular constraint present in the middle of the channel between covalently linked gA peptides.

The starting point for this study is shown in Fig. 1 (redrawn from Cukierman (4)). In this figure, log-log relationships between g_H and $[H^+]$ are shown. The shapes and magnitudes of these plots are different between the S,S- (*blue circles*) and the R,R-dioxolane-linked gA (*red circles*) and native gA channels (*black circles*). Of particular interest is that within the range of $[H^+]$ where H^+ translocation across gA channels seems to be limited by the channel itself (10–2000 mM; see discussions (4,36,41)), the channels have markedly distinct g_H values (4,30,36). The g_H values in the S,S-dioxolane channel are considerably larger and display a power relationship (see legend to Fig. 1) to $[H^+]$ that is absent in other gA channels. The R,R-dioxolane-linked gA channel has the

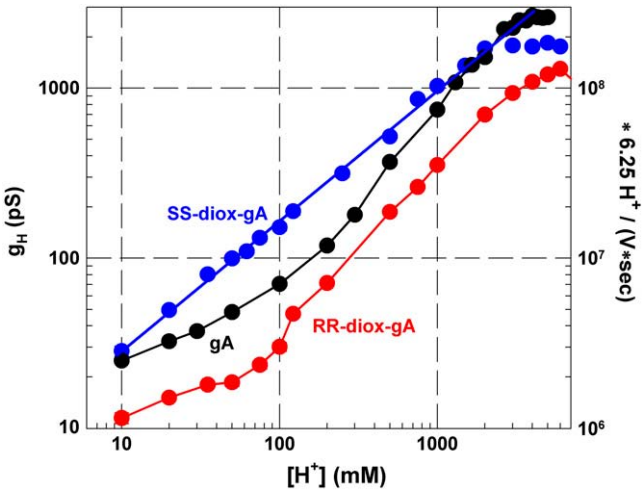

FIGURE 1 Log-log plots of single-channel conductances to H^+ (g_H, pS) or translocation rates of H^+ /(V·s) versus $[H^+]$ (mM). Red, black, and blue symbols and lines correspond to R,R-dioxolane-, native gA, and S,S-dioxolane-linked gA channels, respectively. Means ± SE were plotted in this graph (SE bars are smaller than the size of the symbols). The straight line fitting the blue circles was obtained from linear regression analysis (slope = 0.75). This figure was redrawn from Cukierman (4).

slowest rate of H^+ translocation among the various gA channels thus far studied. This could be caused by the distinct chiralities of two carbons of the dioxolane linker that introduce a major distortion in the secondary structure in the middle of the channel, leading to significant alterations in the H-bond network in that region of the pore (4,27,30,33,37). In this study, this hypothesis is experimentally addressed.

Two major structural differences between native and dioxolane-linked gA channels could account for the differences in the rate of proton transfers (Fig. 1). One relates to the constraint imposed by the five-member dioxolane ring in the middle of the gA channel. The second concerns the presence of oxygens in the dioxolane in the middle of the channel that could be interacting electrostatically with adjacent CO groups of the peptide, and attenuate H^+ translocation in the middle of the channel (4,27,30,33,37).

To address these possibilities, new covalently linked gA channels were synthesized. In Fig. 2 the linkers to which two gA peptides were coupled are shown. The top chemical structure represents the diacid dioxolane linker, and the middle and bottom structures are the diacid cyclopentane and succinic linkers, respectively. Both the S,S- and R,R-dioxolane or cyclopentane linkers were synthesized. The difference between these gA dimers is the absence of two oxygens in the cyclopentane linker, although both S,S rings provide a constrained (considerably fewer degrees of freedom between the two gA peptides as compared to native gA channels (Fig. 3)) continuity between the $\beta^{6,3}$-helices of gA peptides (26, 27,30,32,33). By contrast, in the R,R-dioxolane- or cyclopentane-linked gA channels, the constraint imposed by the 5-member ring is still present between the two gA peptides,

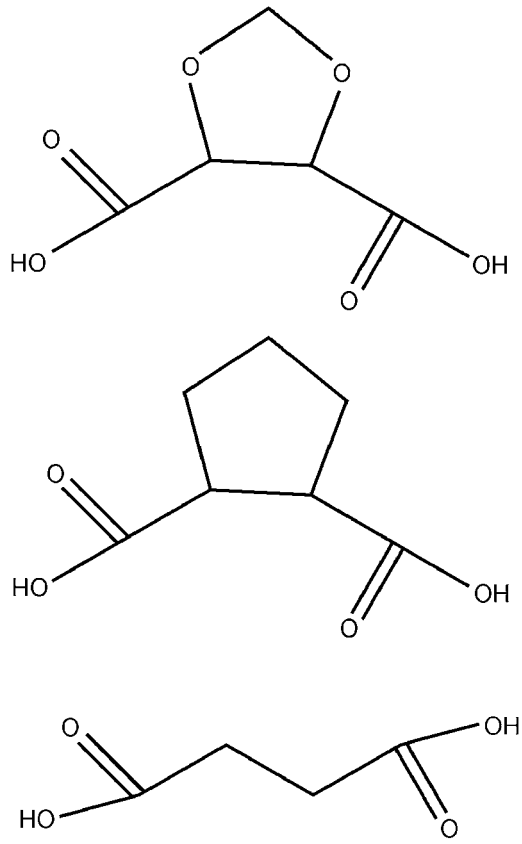

FIGURE 2 The chemical structures of the diacid dioxolane (*top*), diacid cyclopentane (*middle*), and succinic acid (*bottom*) are shown. The formyl group present at the amino terminus of native gA peptides was removed, exposing the terminal NH_2 group that was coupled via a peptide bond to the OH groups in the linkers shown in this figure (see Methods and also Fig. 3).

but a discontinuity in the $\beta^{6.3}$-helices of gA peptides occurs (Fig. 3; 26,27,30,32,33). Succinyl-linked gA channels were also synthesized. In this case, two gA peptides were covalently linked, but a rigid constraint in the middle of the channel is no longer imposed as with either the dioxolane- or cyclopentane-linked gA channels. In Fig. 3, molecular models of the junction between two gA peptides coupled to the various linkers are shown. In this figure the region of the coupling with the linkers is shown from a view inside the channel. Panels in this figure show only the S,S- dioxolane (*A*) and R,R-cyclopentane configurations, which constrain the peptide in relation to the succinyl-linked (*C*) or native gA channels (27,29,30,32,33). The arrows in this figure identify the oxygens in the dioxolane (*A*) and the replacing carbons in the cyclopentane (*B*).

Thus, the comparison between the rates of H^+ translocation in the same stereoisomer of the dioxolane- or cyclopentane-linked gA channel addresses the possible influence of electrostatic interactions caused by the Os in the middle of the channel without eliminating the constraint imposed by the distinct five-member rings.

MATERIAL AND METHODS

Chemistry

Reagents were purchased from Aldrich, Fluka, or Fisher. Some were used as found in the laboratory unless otherwise mentioned. The optical rotations were recorded on a Perkin Elmer 341 automatic Polarimeter using a sodium lamp (λ_D 589 nm). ^1H and ^{13}C NMR spectra were recorded in DMSO-d_6 (deuterated dimethylsulfoxide, δ 2.50 ppm and 39.51 ppm), $CDCl_3$ TMS (tetramethylsilane, δ 0 ppm) with Varian 300- or 400-MHz spectrometers. MS spectra were obtained on a Thermo Finnigan LCQ Advantage and also from Washington University, St. Louis. MALDI (matrix assisted laser desorption ionization) mass spectra data were obtained using either sinnapic acid or α-cyano-4-hydroxy cinnamic acid as the matrix.

HPLC conditions

Reverse-phase Inertsil ODS, a 5-μm, 4.5 $\times$ 150 mm C_{18} column using methanol (MeOH):water (78:22) with 0.005% trifluoroacetic acid (TFA) as the mobile phase at a flow rate of 1.0 ml/min. An SP8800 ternary HPLC pump was used with an Applied Biosystems 783A detector (λ 280 nm) and an Eppendorf column heater. The UV data were obtained on an HP 845x UV-Visible spectrophotometer.

Resolution of *trans*-1,2-cyclopentane dicarboxylic acid

Racemic *trans*-1,2-cyclopentane dicarboxylic acid was resolved by fractional crystallization of the brucine salt, following previous procedures (38). The resolved salts were hydrolyzed to give the S,S and R,R enantiomers. Specific rotations are shown in Table 1.

Preparation of desformyl gA (29, 30)

A 100-mg (53 μmol) sample of commercial gramicidin A (com.gA) was dissolved in 0.8 ml of methanol, with stirring. To this was added a 1.8 ml (5.3 mmol) of 2.98 M anhydrous HCl (freshly prepared reagent). The mixture was stirred at 0° under N_2 for ~2 h. Alternatively, it was also prepared by stirring the mixture at room temperature for 1 h. The mixture was refrigerated for at least 120 h and then placed in the freezer until needed. The solvent was removed on a rotary evaporator to give a white residue, which was suspended in methanol and passed through an AG 11 8A, resin column using methanol followed by 2.0 N NH_4OH in methanol as the eluting solvents. The collected fractions were monitored by UV, and the fractions having the ratio of $A_{282}/A_{246} > 1$ were combined and analyzed by HPLC, NMR, IR, and MS, confirming the presence of the desformyl gA (des.gA). The calculated mass for $C_{98}H_{140}N_{20}O_{16}$ is 1854.28 (measured *m*/z 1855.1 $(M+1)^+$ and 928.1 $(M+2)^{2+}$).

Synthesis of cyclopentane (racemic) diacid gA dimer

A 15.0-mg (8.1 μmol) sample of des.gA was dissolved in 150 μl of dimethylformamide (DMF). To this was added 0.64 mg (4.0 μmol) racemic diacid in 20 μl DMF, followed by 2.0 μl (9.3 μmol) diphenylphosphoryl azide (DPPA) and 1.4 μl (10.1 μmol) triethylamine (TEA). Total volume of DMF used was ~200 μl. All the reagents were added at 0° and stirred under N_2 for ~7 h. The pale orange reaction mixture was placed in the freezer (for at least 4 days) and later quenched with 1.0 ml methanol. The residue obtained after removal of the solvent on the rotary evaporator (residue was not completely dry) was dissolved with 3 $\times$ ~3 ml ethyl acetate (EtOAc). The organic layer was washed with 5 ml aqueous 0.1 N $KHCO_3$, 5 ml aqueous 0.1 N $NaHSO_4$, and 2 $\times$ 5 ml D.I water. The organic layer was

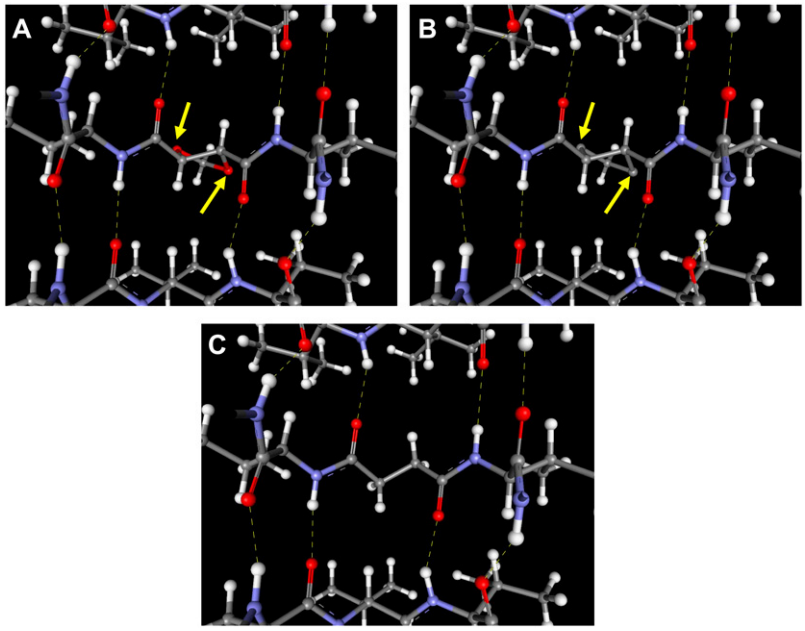

FIGURE 3 This figure shows the junction of two gA peptides via an S,S-dioxolane (*A*), S,S-cyclopentane (*B*), and succinyl (*C*) linkers. The views in this figure are from inside the middle of the channels, where linkers are coupled to desformylated gA peptides. The orientation of the channels in this figure is such that their extremities extend to the top and bottom directions in the figure. Arrows in *A* and *B* identify the oxygens (*A*) and carbons (*B*) in the distinct linkers. For the sake of clarity, the hydrogens in the carbons replacing the oxygens (*arrows in B*) were removed. Notice the constraints caused by the five-member ring (*A* and *B*) and its lack with the succinyl linker (*C*). These distinct channels were energy minimized using molecular mechanics and following standard procedures previously described (27,30).

dried with anhydrous $MgSO_4$ to give 10.9 mg (~68% yield) of the solid product. HPLC, NMR, UV, and MS data for the purified dimer were obtained, and that supported the presence of gA dimer. Calculated mass was $C_{203}H_{286}N_{40}O_{34}$ 3831.28, and the observed was 3831.1 (LC-MS data) $(M+1)^+$ and 3853.33 $(M+Na)^+$ (MALDI with sinnapic acid).

Synthesis of S,S-cyclopentane diacid gA dimer

The S,S-cyclopentane diacid was isolated from the diastereomeric brucine (38) salt having a specific rotation of $-16.2° \pm 0.2°$) through fractional crystallization. The specific rotation for the isolated S,S-diacid in water was $+44.1° \pm 0.2°$. The procedure for dimer synthesis was same as mentioned above. HPLC, NMR, UV, and MS data for the purified dimer were obtained, and they supported the presence of the gA dimer. Calculated and measured masses for $C_{203}H_{285}N_{40}O_{34}Na$ were 3854.28 and 3853.72 $(M+Na)^+$ (MALDI with sinnapic acid), respectively.

Synthesis of R,R-cyclopentane diacid gA dimer

The R,R-cyclopentane diacid used isolated from the diastereomeric brucine salt having a specific rotation of $-34.7° \pm 0.3°$ through fractional crystallization. The specific rotation for the isolated R,R-diacid in water was found to be $-87.6° \pm 0.2°$. The procedure for the dimer synthesis was as mentioned above. HPLC data for the R,R dimer were obtained. Calculated and measured masses for $C_{203}H_{285}N_{40}O_{34}Na$ were 3854.28 and 3855.15 $(M+Na)^+$ (MALDI with sinnapic acid), respectively.

TABLE 1 Specific rotations of S,S (upper row) and R,R (bottom row) *trans*-1,2-cyclopentane dicarboxylic acid ($[\alpha]_D$ at 589 nm)

Our study		Literature (38)	
Salt	Acid	Salt	Acid
-34.7 ± 0.3	-87.6 ± 0.2	-26.6	-85.9
-16.2 ± 0.2	$+44.1 \pm 0.2$	-19.9	$+87.6$

Synthesis of succinyl-linked gA dimer

A 5.9-mg (3.18 μmol) sample of des.gA was dissolved in 50 μl of DMF. To this was added 0.176 mg (1.49 μmol) succinic acid in 3.10 μl DMF, followed by 0.80 μl (3.71 μmol) DPPA and 0.80 μl (5.72 μmol) TEA. Total volume of DMF used was ~165 μl. All the reagents were added at 0° and stirred under N_2 for ~7 h. The reaction mixture was placed in the freezer until needed. HPLC data were obtained for the dimer.

Planar lipid bilayers

The experimental chamber consisted of two polystyrene aqueous compartments separated by a partition containing a 0.10- to 0.15-mm diameter hole. Planar lipid bilayers were formed by the painting technique onto the hole from a 60 mM stock solution of monoolein (Δ9-*cis*-glyceryl-monoolein, GMO) in decane. The formation (thinning) of a lipid bilayer was monitored visually and by measuring the bilayer capacitance. The leak resistance of the planar bilayers used in this study in various HCl solutions was larger than 30 GΩ.

Solutions and ion channels

Experiments were performed with symmetrical solutions of HCl of various concentrations across the lipid bilayer. All experiments were performed at room temperature (22°–24°). Distinct ion channels were used in this study. They were added from a methanol solution to only one side (*cis*-side) of the bilayer. While native gA was added at a final concentration of $\sim 10^{-9}$ M to the *cis*-side of the chamber, the dimerized gA channels were added at a considerably lower concentration ($\sim 10^{-11}$ M). A single experiment consisted of recording the single-channel conductances to protons (g_H) of various channels (5–15) incorporated into the bilayer. This procedure was repeated many times after thorough cleaning of the experimental chambers. From the point of view of gathering g_H data, it was more efficient to characterize the cyclopentane-linked gA channels in lipid bilayers using their racemic mixture. However, and as demonstrated in Fig. 4, the final confirmation of the peaks in the bigaussian distribution of g_H values was performed using only the individual S,S- or R,R-cyclopentane-linked gA channels.

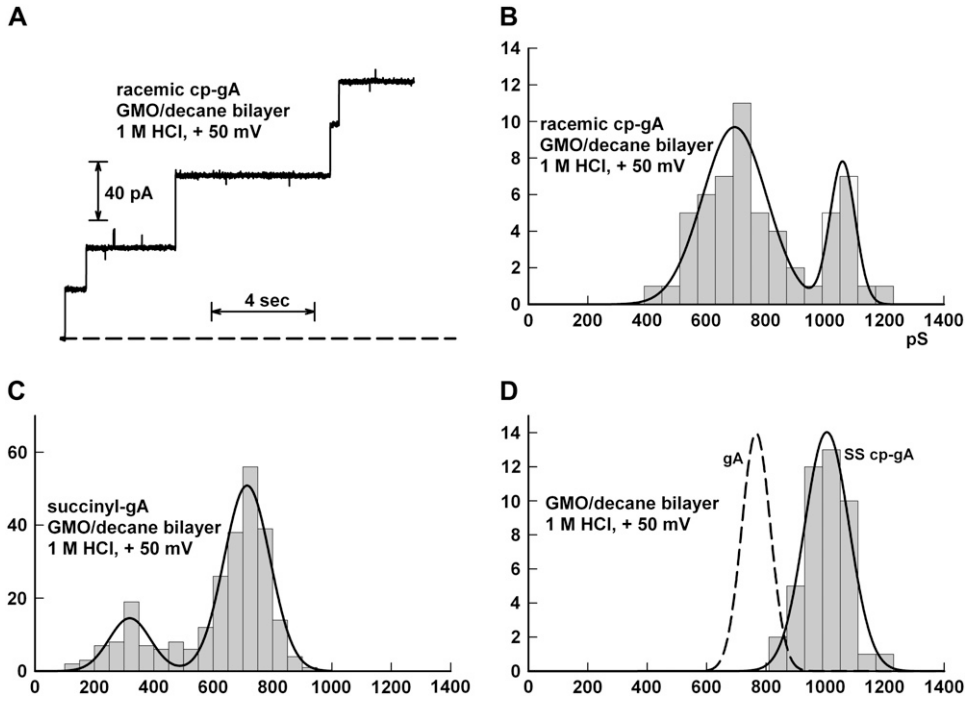

FIGURE 4 Experimental approach for the determination of g_H values in the various covalently linked gA channels. (*A*) Single-channel recordings in a GMO bilayer in symmetrical 1 M HCl solutions at room temperature and at a transmembrane voltage of 50 mV. The original recording (low-pass Bessel filtered at 5 kHz) was digitally filtered at 100 Hz, and the number of points reduced 20-fold for illustration purposes only. Racemic cyclopentane-linked gA channels were added in a methanol solution to the *cis*-side of the bilayer at a final concentration ~20–50 pM. The dashed line represents the baseline (0 pA). Upward deflections in the recording indicate incorporations of a channel in the open state into the bilayer. Notice that the channels remained in the open state throughout the duration of this recording (see below), which does not occur with native gA channels (4,29–31,34–36). (*B*) Histogram distributions of g_H values as measured in several experiments such as the one shown in panel *A*. Bigaussian distributions were fitted to the histograms with means of 695.1, and 1058.8 pS. (*C*) As in *B* but with succinyl-linked gA channels (means of 319.4 and 714.3 pS, see text for discussion). (*D*) Distribution of g_H for native gA channels (*dashed curve*), and S,S-cyclopentane-linked gA channels (*continuous curve*). The mean values for those peaks are 747.1 pS (gA) and 1015.2 pS (S,S-cyclopentane-linked gA channels). The number of g_H measurements with gA channels only was much larger than shown by the dashed curve, which was normalized to provide a peak with similar amplitude as with S,S-cyclopentane-linked gA channels. Notice that the second larger peak in the histogram distribution in panel *B* is in agreement with experimental measurements with only the S,S-cyclopentane-linked gA channels in this panel. It is essential to notice that under the experimental conditions of this figure, native gA channels have an average open time duration of 3.98 ± 0.33 s ($n = 133$). Only covalently linked gA channels whose open times lasted longer than 25 s had their g_H values computed. With this procedure, the unlikely possibility of contamination of recordings of covalently-linked gA channels with native gA channels was basically eliminated.

Electrical measurements and analyses

An Ag/AgCl electrode in virtual ground configuration applied transmembrane potentials and recorded single-channel currents in the *cis*-side of the bilayer. The *trans*-side was grounded via Ag/AgCl electrodes. A patch-clamp amplifier (Axopatch 2B, Axon Instruments, Union City, CA) was used in this procedure. Single-channel events were recorded after low-pass Bessel filtering at 5 kHz, digitized (at 20 kHz), and analyzed using pClamp software (Axon Instruments). A recording of one experiment is shown in Fig. 4 *A*.

RESULTS AND DISCUSSION

Fig. 4 *A* shows a continuous electrical recording in which five cyclopentane-linked gA channels incorporated into a GMO/decane bilayer in symmetrical solutions of 1 M HCl. In this recording the racemic mixture of S,S- and R,R-cyclopentane channels was used. Fig. 4 *B* shows the corresponding histogram distribution of g_H values measured in various experiments (distinct bilayers) as in Fig. 3 *A*. The distribution of the measured g_H values has always displayed a bigaussian distribution with two well-defined distinct peaks with the racemic mixture of the S,S- and R,R-cyclopentane channels. The peaks corresponding to the larger and smaller g_H values were identified as corresponding to the S,S- and R,R-cyclopentane-linked gA channels, respectively. This is demonstrated in panel *D* of Fig. 4. This histogram shows g_H measurements of the S,S-cyclopentane-linked gA channels only. Notice that the peak of this single Gaussian distribution is in excellent agreement with the peak with the highest g_H value in the bigaussian distribution of Fig. 3 *B*. This has been the case under various $[H^+]$. Also illustrated in Fig. 3 *D* is the histogram distribution for g_H values in native gA channels. Notice that the mean g_H of native gA channels is close to the one in the R,R-cyclopentane-linked gA channels. In this context it is important to allay concerns related to contamination of native gA channels with our covalently linked gA channels. 1), Native gA peptides were desformylated at a yield >95%. Desformylated gA peptides do not form ion channels in lipid bilayers (S. Cukierman, unpublished observations). 2), Under the experimental conditions of this figure, native gA channels have an average open time duration of 3.98 ± 0.33 s ($n = 133$). Only covalently linked gA channels whose open times lasted longer than 25 s had their g_H values computed. With this procedure, the unlikely possibility of contamination of recordings of covalently linked gA channels with native gA channels was basically eliminated (Fig. 3).

In Fig. 4 *C* the distribution of g_H values for the succinyl-linked gA channels under the same experimental conditions

as previous histograms and recordings is illustrated. In this case, a wide distribution of g_H values (100–1000 pS) that is also well represented by a bigaussian distribution in a wide range of $[H^+]$ was observed. This is in sharp contrast with our previous experimental observations with native gA and various other gA dimer channels (4,29–31,34–36,39). Interestingly, there is no interconversion between distinct g_H values once a given succinyl-linked gA channel incorporates into the bilayer; i.e., once a succinyl-gA channel incorporates in the bilayer, its g_H remains unchanged. This experimental conclusion (time-independent change of g_H for a channel incorporated into the bilayer) also holds for other types of covalently linked gA channels used in this as well as in previous studies.

The measurements illustrated in Fig. 4 were performed in a wide range of $[H^+]$ for the cyclopentane- and succinyl-linked channels, and the results are summarized in the log (g_H)–log ($[H^+]$) plots of Fig. 5. In this figure, the blue, black, and red lines are the same as in Fig. 1 and refer to the S,S- and R,R-dioxolane-linked and native gA channels, respectively. The triangles and squares represent measurements from the S,S- and R,R-cyclopentane-linked gA channels, respectively, and open circles are the peaks of the bigaussian distributions for the succinyl-linked gA channels.

The experimental points for the S,S-cyclopentane-linked channel (*triangles*) are well fitted by the straight line that is representative of the experimental points for the S,S-dioxolane-linked gA channels (Fig. 1). This result suggests that a continuous and constrained transition between the two gA peptides via either the S,S-dioxolane or cyclopentane linkers enhances the rate of H^+ transfer in the middle of the channel by about two- to fourfold relative to native gA

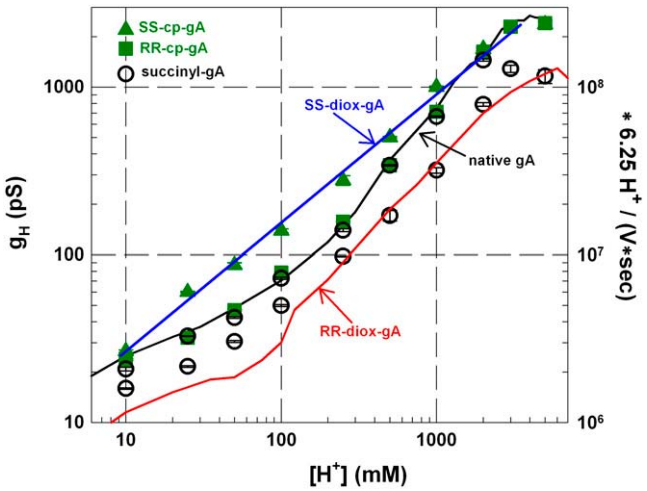

FIGURE 5 Red, black, and blue lines are from Fig. 1 and correspond to experimental measurements of g_H in the R,R-dioxolane, native gA, and S,S-dioxolane-linked gA channels, respectively. Green triangles and squares are g_H values for the S,S- and R,R-cyclopentane-linked gA channels, respectively. Open circles were measured in succinyl-linked gA channels. Means ± SE were plotted in this graph.

channels and in the range of $[H^+]$ 10–1000 mM. Additional support for this idea comes from the larger peak of the bimodal distribution of g_H values for the succinyl-linked gA channels (*open circles* in Fig. 5; see also Fig. 4C) which are in excellent agreement with the experimental measurements in native gA and are significantly lower than g_H values in the S,S-linked cyclopentane or dioxolane channels. Disruption of the five-member ring of channels (cyclopentane or dioxolane linked) makes the channel transfer H^+ at the same rate as in native gA channels, albeit with a wide distribution of gA values (see below). Moreover, these experimental results suggest the lack of significant electrostatic interactions between oxygens of the dioxolane and the first CO groups of gA peptides on the rate of H^+ transfer in S,S-dioxolane (27,37).

It has been previously shown that a significant entropic component underlies the quantitative differences between the rate of H^+ transfer in native and dioxolane-linked gA channels (34). This can be reasoned by assuming that H^+ transfer in a Grotthuss-like mechanism is greatly dependent on appropriate geometric (or electrostatic) relationships between water molecules that in turn interact with the carbonyls from gA that protrude into the lumen of the pore (4,19,26, 27,37). Thermal fluctuations of the membrane-protein complex cause significant alterations in the structure of the water wire in the middle of native gA channels (4,26,27,34,35, 39,40). It is likely that in some of these temporary water wire structures, H^+ transfer (via either the hopping or the turn steps) in the middle of the channel may be hampered or even interrupted, thus decreasing the overall rate of H^+ translocation across the channel. By providing a continuous and constrained transition between the two gA peptides, both the S,S-dioxolane and S,S-cyclopentane rings cause an increased order in the structure of the water wire in the middle of the channel that is more favorable for H^+ transfer. This increased order (as it favors proton transfer) in the water wire structure in the S,S dimers could be a consequence of reducing the number of degrees of freedom that are normally present when native channels are simply formed by an apposition of the N-termini of two gramicidin A peptides via H bonds (unconstrained configuration). This association may occur under different structural arrangements between the gA peptides, and this may well originate a number of distinct water wire structures. Some of these water wire structures may not be as optimally suited to transfer protons as in the S,S gA dimers. This would explain the enhancement of g_H in S,S-dioxolane-linked gA channels in relation to native or even R,R-dioxolane-linked gA channels (see below). It is of interest to notice that at in the range of $[H^+] < 10$ mM and $>$ 2000 mM in which diffusion limitation of H^+ to and from the channel seems to have a more significant role in H^+ translocation across the channel (4,36,41), the S,S-linked channels and native gA channels have relatively small differences between their g_H values.

Although the S,S-dioxolane- and cyclopentane-linked channels are indistinguishable in regard to their H^+ transfer

properties, the same does not apply to their R,R counterparts. Replacing the oxygens by carbons in the R,R-dioxolane significantly enhances the H^+ translocation across the water wire in channels. In fact, the R,R-dioxolane ''becomes'' functionally equivalent to native gA channels at least in relation to g_H (interestingly, this statement does not hold for Cs^+ and K^+ permeation (D. L. Wyatt and S. Cukierman, unpublished data)). This is shown in Fig. 5 in which the green squares corresponding to the R,R-cyclopentane-linked channel depart significantly from the red line that represents the R,R-dioxolane-linked gA channels and are well fitted by the black line of native gA channels.

It has been suggested that the significant attenuation in the translocation of protons in the R,R-dioxolane-linked gA channels is caused by a significant distortion in the secondary structure in the middle of the channel (4,27,30). In a subsequent molecular dynamics study, it was reasoned that in the R,R-dioxolane-linked gA channel (but not in the S,S-dioxolane-linked or native gA channels) an electrostatic mechanism (named the molecular ''switch'') in the middle of the channel accounts for the delayed transfer of protons in the middle of the pore (37). In particular, the projection inside the lumen of the channel of the carbonyls of valines flanking the R,R-dioxolane linker favors the local H^+ transfer. There exists a dynamics between the two carbonyls flanking the R,R-dioxolane pointing in and out of the pore (in/in, in/out, out/in, out/out), and H^+ transfer is favored by an in/out or out/in conformation. As a consequence of this dynamics, nanosecond delays in the local rate of proton transfer can be introduced in the middle of the channel. Said dynamics of carbonyl pointing in or out of the pore is likely to be a consequence of electrostatic interactions between the dioxolane oxygens and carbonyl oxygens in the valines caused by local distortions in the secondary structure in the middle of channels.

Similar distortions in the secondary structure in the middle of the channel seem to occur for both the R,R-dioxolane- and R,R-cyclopentane-linked gA channels (Fig. 2). However, the lack of oxygens in the latter eliminates the possible electrostatic interactions described above. This could eliminate the delay in the transfer of protons in the middle of R,R-dioxolane-linked channels, thus enhancing g_H (37). The fact that g_H values in the R,R-cyclopentane channel are substantially larger than those in their dioxolane counterpart provides encouragement for this hypothesis. It would be highly instructive to perform molecular dynamics simulations in the R,R-cyclopentane-linked gA channels using distinct methodologies (12,13).

In previous studies, the structure of the S,S-dioxolane-linked gA dimer has been considered similar to native gA channels (27,30,32,33,37). Interestingly, and at least in relation to g_H, the R,R-cyclopentane gA dimer is functionally more representative of native gA channels than the S,S-linked gA dimers. This questions whether the association between two native gA peptides via H bonds in the middle of the bilayer should really be idealized as having a continuous and frozen transition in the middle of the channel. This questioning finds interesting support in recent calculations in which the fluctuation dynamics of membrane channels influences appreciably the free energy barrier for proton permeation inside various gA channels (40). It is likely that there are several ''structures'' of native gA channels inside the membrane, each having its own specific pattern for ion permeation.

Compared to other studied gA channels, succinyl-linked channels have a very wide distribution of g_H values (Fig. 4 *C*). These values range from ~100 pS to ~1000 pS. By contrast, all other gA channels studied have a narrower range of g_H values (see for example Fig. 4 *D*). This has also been shown for glutaryl-linked gA channels (S. Cukierman, unpublished observations). Interestingly, the g_H of a given incorporated succinyl-linked channel is invariant, suggesting that the population of configurations of the channel and water wire is maintained inside the bilayer after incorporation (see previous paragraph). Compared to other gA channels (including the native), the wide distribution of g_H values is explained by the distinct possible conformations of the succinyl group in the middle of the channel causing distinct water wire structures, some of them not ideal for localized proton transfer. A bigaussian represented the distribution of g_H in succinyl-linked gA channels with the larger peak being quite similar to g_H in native gA (or the R,R-cyclopentane-linked channels) and the lower peak similar, at least at some $[H^+]$, to g_H values in the R,R-dioxolane-linked gA channels. This channel offers an interesting opportunity to establish relationships among the various structures of the channel, water wires, and proton transfer. Furthermore, these findings suggest that constraining a continuous transition between the two gA peptides (S,S-linked channels) enhances the rate of H^+ transfer in water wires by decreasing the number of configurations of water wires that are not ideal for transferring protons inside the channel (decrease in the activation entropy (34)).

CONCLUDING REMARKS

Ion channels formed by gramicidin A peptides offer an excellent opportunity to probe and understand the transfer of protons in quasiunidimensional water wires. It has been previously demonstrated that linking two gA peptides with an S,S- (or R,R-) dioxolane enhances (or attenuates) H^+ transfer in relation to native gA channels, which themselves are formed by the association of two gA peptides via H bonds (4,29–31,34–36,39). In this study, the molecular basis of these effects was explored by replacing the dioxolane either by a cyclopentane or by a succinyl linker. A suitable configuration of water molecules is an essential requirement for H^+ to be transferred between two adjacent water molecules in a water wire (12,13,26–28,37). Thermal fluctuations of the membrane-gA complex (40) are likely to originate

distinct dynamic structures of water wires. In some of these structures, proton transfer will occur faster than in others. In some of water wire structures, proton transfer may not even occur. Consequently, g_H represents a time average of distinct rates of proton transfer in the various configurations of water wires. One conclusion from this study is that a constrained and continuous transition between two gA peptides (via either a S,S-dioxolane or cyclopentane linkers) would favor conformations of water wires that transfer protons at a higher rate (in relation to native gA channels) via a reduction in the activation entropy (34). On the other hand, previous computational studies of R,R-dioxolane-linked gA channels suggested that the projections of carbonyls adjacent to the R,R-dioxolane linker into the lumen of the channel pore could introduce a nanosecond delay in proton transfer in the middle of the channel (27,37). This electrostatic effect could account for the reduced g_H in the R,R-dioxolane-linked gA channels compared to native gA channels. When the oxygens of the dioxolane linker were replaced by carbons (R,R-cyclopentane-linked gA channels), the attenuation of g_H was no longer observed, thus providing support for the hypothesis previously advanced.

It should be mentioned finally that the experimental approach used in this study consisted of replacing a few atoms in an ion channel and measuring the resultant change in its function. In terms of structure-function relations, this experimental approach appears to be more directly or easily interpretable, and perhaps even more illuminating, than swapping entire amino acids or their sequences. The experimental data generated using this strategy will also contribute to the further development of more accurate and insightful MD studies.

This work was supported by National Institutes of Health (RO1GM59674).

REFERENCES

1. Cukierman, S. 2003. The transfer of protons in water wires inside proteins. *Front. Biosci.* 8:1118–1139.
2. Cukierman, S. 2006. Et tu Grotthuss! and other unfinished stories. *Biochim. Biophys. Acta (Bioenergetics).* 1757:876–885.
3. DeCoursey, T. E. 2003. Voltage-gated proton channels and other proton transfer pathways. *Physiol. Rev.* 83:475–579.
4. Cukierman, S. 2000. Proton mobilities in water and in different stereoisomers of covalently linked gramicidin A channels. *Biophys. J.* 78: 1825–1834.
5. Grotthuss, C. J. T. 1806. Sur la décomposition de l'eau et des corps qu'elle tient en dissolution à l'aide de l'électricité galvanique. *Ann. Chim.* LVIII:54–74.
6. Bernal, J. D., and R. H. Fowler. 1933. A theory of water and ionic solution, with particular reference to hydrogen and hydroxyl ions. *J. Chem. Phys.* 1:515–548.
7. Conway, B. E. 1964. Proton solvation and proton transfer processes in solution. *In* Modern Aspects of Electrochemistry, Vol. 3. J. O. M. Bockris and B. E. Conway, editors. Butterworths, London. 43–148.
8. Eigen, M. 1964. Proton transfer, acid-base catalysis, and enzymatic hydrolysis. *Ang. Chem.* 3:1–72.
9. Nagle, J. F., and H. J. Morowitz. 1978. Molecular mechanisms for proton transport in membranes. *Proc. Natl. Acad. Sci. USA.* 75:298–302.
10. Agmon, N. 1995. The Grotthuss mechanism. *Chem. Phys. Lett.* 244: 456–462.
11. Day, T. J. F., U. W. Schmitt, and G. A. Voth. 2000. The mechanism of hydrated proton transfer in water. *J. Am. Chem. Soc.* 122:12027–12028.
12. Voth, G. A. 2006. Computer simulation of proton solvation and transport in aqueous and biomolecular systems. *Acct. Chem. Res.* 39: 143–150.
13. Swanson J. M. J., C. M. Maupin, H. Chen, M. K. Petersen, J. Xu, Y. Wu, and G. A. Voth. 2007. Proton solvation and transport in aqueous and biomolecular systems: Insights from computer simulations. *J. Phys. Chem. B.* 111:4300–4314.
14. Warshel, A. 2003. Computer simulation of enzyme catalysis: Methods, progress, and insights. *Annu. Rev. Biophys. Biomol. Struct.* 32:425–443.
15. Lapid H., N. Agmon, M. K. Petersen, and G. A. Voth. 2005. A bond-order analysis of the mechanism for hydrated proton mobility in liquid water. *J. Chem. Phys.* 122, 014506.
16. Sarges, R., and B. Witkop. 1965. V. The structure of valine- and isoleucine-gramicidin A. *J. Am. Chem. Soc.* 87:2011–2019.
17. Urry, D. W. 1971. Gramicidin A transmembrane channel: a proposed $\pi_{(L,D)}$ helix. *Proc. Natl. Acad. Sci. USA.* 68:672–676.
18. Urry, D. W., M. C. Goodall, J. D. Glickson, and D. F. Meyers. 1971. The gramicidin A transmembrane channel: characteristics of head-to-head dimerized $\pi_{(L,D)}$ helices. *Proc. Natl. Acad. Sci. USA.* 68: 1907–1911.
19. Arseniev, A. S., I. L. Barsukov, V. F. Bystrov, A. L. Lonize, and Y. A. Ovchinikov. 1985. Proton NMR study of gramicidin A transmembrane ion channel. Head-to-head right handed, single stranded helices. *FEBS Lett.* 186:168–174.
20. Cross, T. A. 1997. Solid-state nuclear magnetic resonance characterization of gramicidin channel structure. *Meth. Enzymol.* 289:672–696.
21. Hladky, S. B., and D. A. Haydon. 1972. Ion transfer across lipid membranes in the presence of gramicidin A. I. Studies of the unit conductance channel. *Biochem. Biophys. Acta.* 274:294–312.
22. Andersen, O. S. 1984. Gramicidin channels. *Annu. Rev. Physiol.* 46: 531–548.
23. Busath, D. D. 1993. The use of physical methods in determining gramicidin channel structure and function. *Annu. Rev. Physiol.* 55: 473–501.
24. Levitt D.G. 1984. Kinetics of movement in narrow channels. *Curr. Top. Memb. Transp.* 21:181–197.
25. Finkelstein, A. 1987. Water Movement through Lipid Bilayers, Pores, and Plasma Membrane. Theory and Reality. John Wiley & Sons, New York.
26. Pomès, R., and B. Roux. 1996. Structure and dynamics of a proton wire: a theoretical study of H^+ translocation along the single-file water chain in the gramicidin A channel. *Biophys. J.* 71:19–39.
27. Yu, C. H., S. Cukierman, and R. Pomès. 2003. Theoretical study of the structure and dynamic fluctuations of dioxolane-linked gramicidin channels. *Biophys. J.* 84:816–831.
28. Sagnella, D. E., and G. A. Voth. 1996. Structure and dynamics of hydronium in the ion channel gramicidin A. *Biophys. J.* 70:2043–2051.
29. Cukierman, S., E. P. Quigley, and D. S. Crumrine. 1997. Proton conduction in gramicidin A and in its dioxolane-linked dimer in different lipid bilayers. *Biophys. J.* 73:2489–2502.
30. Quigley, E. P., P. Quigley, D. S. Crumrine, and S. Cukierman. 1999. The conduction of protons in different stereoisomers of dioxolane-linked gramicidin A channels. *Biophys. J.* 77:2479–2491.
31. Armstrong, K. M., E. P. Quigley, P. Quigley, D. S. Crumrine, and S. Cukierman. 2001. Covalently linked gramicidin channels: effects of linker hydrophobicity and alkaline metals on different stereoisomers. *Biophys. J.* 80:1810–1818.
32. Stankovic, C. J., S. H. Heinemann, J. M. Delfino, F. J. Sigworth, and S. L. Schreiber. 1989. Transmembrane channels based on tartaric acid-gramicidin A hybrids. *Science.* 244:813–817.

33. Crouzy, S., T. B. Woolf, and B. Roux. 1994. A molecular dynamics study of gating in dioxolane-linked gramicidin A channels. *Biophys. J.* 67:1370–1386.

34. Chernyshev, A., and S. Cukierman. 2002. Thermodynamic view of activation energies of proton transfer in various gramicidin A channels. *Biophys. J.* 82:182–192.

35. Chernyshev, A., R. Pomès, and S. Cukierman. 2003. Kinetic isotope effects of proton transfer in aqueous and methanol containing solutions, and in gramicidin channels. *Biophys. Chem.* 103:179–190.

36. Chernyshev, A., and S. Cukierman. 2006. Proton transfer in gramicidin channels in phospholipid membranes. Attenuation by phosphoethanolamine headgroups. *Biophys. J.* 91:580–587.

37. Yu, C. H., and R. Pomès. 2003. Functional dynamics of ion channels: modulation of proton movement by conformational switches. *J. Am. Chem. Soc.* 125:13890–13894.

38. Goldsworthy, W. L., W. Henry, and J. Perkin. 1914. Resolution of *trans*-cyclopentane-1,2-dicarboxylic acid. *J. Chem. Soc.* 105:2639–2643.

39. Armstrong, K. M., and S. Cukierman. 2002. On the origin of closing flickers in gramicidin channels: a new hypothesis. *Biophys. J.* 82:1329–1337.

40. Qin, Z., H. L. Tepper, and G. A. Voth. 2007. Effect of membrane environment on proton permeation through gramicidin A channels. *J. Phys. Chem. B.* In press.

41. Quigley, E. P., A. Emerick, D. S. Crumrine, and S. Cukierman. 1998. Proton current attenuation by methanol in a dioxolane-linked gramicidin A dimer in different lipid bilayers. *Biophys. J.* 5:2811–2820.